

# Altered processing of Alzheimer amyloid precursor protein in response to neuronal degeneration

(dementia/proteolysis)

KERSTIN IVERFELDT\*, S. IVAR WALAAS†, AND PAUL GREENGARD\*‡

\*Laboratory of Molecular and Cellular Neuroscience, The Rockefeller University, New York, NY 10021; and †Neurochemical Laboratory, University of Oslo, 0317 Oslo 3, Norway

Contributed by Paul Greengard, January 28, 1993

**ABSTRACT** In the brains of individuals with Alzheimer disease, senile plaques containing aggregates of  $\beta$ -amyloid peptide, derived from the  $\beta$ -amyloid precursor protein (APP), are seen in association with degenerating nerve terminals. It is not known whether the degenerating nerve terminals cause the formation of these aggregates or whether  $\beta$ -amyloid peptide in the aggregates causes nerve-terminal degeneration. In the present study of rat brain, degeneration either of local neurons or of nerve terminals caused decreased levels of a neuron-enriched isoform of APP, increased levels of a glia-enriched isoform of APP, and increased levels of potentially amyloidogenic, as well as nonamyloidogenic, COOH-terminal fragments of APP. Our results demonstrate that neuronal degeneration affects APP processing and suggest that it may contribute to amyloid formation in mammalian brain.

$\beta$ -Amyloid precursor protein (APP) is a transmembrane glycoprotein that exists as three major isoforms, APP<sub>695</sub>, APP<sub>751</sub>, and APP<sub>770</sub> (the subscripts refer to the number of amino acids), which are encoded by a single gene (1–7). APP undergoes posttranslational processing that includes maturation (i.e., glycosylation and sulfatation) and proteolytic cleavage, which generates peptide fragments such as  $\beta$ -amyloid ( $\beta$ /A4). Deposits of  $\beta$ /A4 are found within the senile plaques in the brains of patients with Alzheimer disease.  $\beta$ /A4 is believed to be a factor in the etiology of the disease. The mechanisms responsible for APP processing are incompletely understood. Chemical lesioning of nerve cell bodies is accompanied by an increase in APP immunostaining near the lesion: increased APP immunoreactivity has been reported in neurites and astroglial cells (8, 9) as well as in neurites and microglia/macrophages (10). However, the effect of such lesioning on the processing of APP in affected areas has not been elucidated. Lesioning of the cholinergic input to the cerebral cortex was reported to increase the rate of APP synthesis *in vitro*; however, no changes in the APP levels were detected (11).

In the present study, we have examined the effect of neuronal lesioning on the levels of full-length APP and proteolytic fragments both in proximity to the lesion and in distal projection areas.

## MATERIALS AND METHODS

Affinity-purified rabbit anti-COOH-terminal APP antibody 369 (12), dopamine- and cAMP-regulated phosphoprotein of  $M_r$  32,000 (DARPP-32) monoclonal antibody, clone 5a (13), and rabbit anti-synapsin I antiserum 454/455 (14) have been described. Glial fibrillary acidic protein (GFAP) monoclonal antibody, clone G-A-5, was purchased from Sigma. Anti-Kunitz protease inhibitor (KPI)-domain monoclonal anti-

body 56.1 (15) was from T. V. Ramabhadran (our laboratory). CT15, antiserum raised against the COOH-terminal 15 amino acids of APP, was from E. H. Koo (Harvard Medical School, Boston). Affinity-purified rabbit anti-mouse IgG was obtained from Cappel Laboratories.

Rats of both sexes (150–200 g) were anesthetized by i.p. administration of fentanyl (Hypnorm, 0.1 ml; Janssen, Belgium) and diazepam (Valium, 0.05 ml; Hoffmann-LaRoche), placed in a stereotaxic frame, and subjected either to stereotaxic infusion of quinolinic acid (200 nmol in 2  $\mu$ l, adjusted to pH 7.4 with NaOH) into the neostriatum (16) or to suction lesions of the anterior cerebral cortex (17). Seven days postsurgically, the rats were decapitated, and brain regions both ipsilateral (lesion) and contralateral (control) to the lesions were dissected and rapidly frozen in liquid N<sub>2</sub>. The samples were homogenized by sonication in boiling 1% (wt/vol) NaDodSO<sub>4</sub>, and protein content was determined (18). Samples containing equal amounts of protein were subjected to NaDodSO<sub>4</sub>/PAGE with 5–17.5% gradient gels in Tris/glycine (19) or in Tris/tricine (20) buffer. Proteins were electrotransferred to nitrocellulose sheets and probed with antibodies. The nitrocellulose sheets probed with APP antibodies were incubated with horseradish peroxidase-coupled secondary antibody (Amersham). APP immunoreactivity was detected by using enhanced chemiluminescence (ECL; Amersham) and quantitated by scanning densitometry. The nitrocellulose sheets probed with DARPP-32 and GFAP antibodies were incubated with rabbit anti-mouse IgG (1:500 dilution). Secondary antibodies and synapsin I antibody were labeled by <sup>125</sup>I-labeled protein A overlay, and protein bands were quantitated by PhosphorImager (Molecular Dynamics, Sunnyvale, CA).

For clarity of presentation, in Figs. 1A, 4A, and 5, arrows point only to those immunoreactive bands the intensities of which were altered by lesioning. Data obtained in lesioned material from each animal were expressed as percentage of values obtained in the contralateral control side. Samples from nonlesioned animals, analyzed in parallel, gave results similar to those obtained with the control samples.

## RESULTS

**Identification of APP Species.** Full-length APP molecules from mammalian brain migrate as a group of proteins with apparent molecular masses between 100 and 135 kDa, when analyzed by NaDodSO<sub>4</sub>/PAGE (21–25). Using antiserum 369, directed against the COOH terminus of APP, we observed several APP species in the neostriatum of untreated

Abbreviations: APP,  $\beta$ -amyloid precursor protein;  $\beta$ /A4,  $\beta$ -amyloid; KPI, Kunitz-type protease inhibitor; APP<sub>KPI</sub>, isoform(s) of APP containing a KPI domain; DARPP-32, dopamine- and cAMP-regulated phosphoprotein of  $M_r$  32,000; GFAP, glial fibrillary acidic protein.

‡To whom reprint requests should be addressed.

The publication costs of this article were defrayed in part by page charge payment. This article must therefore be hereby marked "advertisement" in accordance with 18 U.S.C. §1734 solely to indicate this fact.

rats: one distinct band with an apparent molecular mass of 106 kDa, at least two less-distinct bands of 112 and 120 kDa, low levels of a 139-kDa band, and a fragment of 15 kDa (Fig. 1). The 106-kDa band in rat brain comigrated with an APP immunoreactive band from PC-12 cells (26) identified as immature APP<sub>695</sub>, and the 139-kDa band comigrated with a band from PC-12 cells (26) identified as mature APP<sub>751</sub> (data not shown). The 139-kDa band was also recognized by antibody 56.1, which was raised against the KPI domain of APP<sub>751</sub> and APP<sub>770</sub> (15). Additional KPI-containing APP isoforms (L-APP<sub>733</sub> and L-APP<sub>752</sub>) have been reported (27), which would not be readily distinguishable from APP<sub>751</sub> by using the present experimental conditions. Therefore, the bands that comigrate with APP<sub>751</sub> and cross-react with antibody 56.1 are referred to as APP<sub>KPI</sub>. The two less-distinct bands of 112 kDa and 120 kDa most likely represent immature APP<sub>KPI</sub> and mature APP<sub>695</sub>, respectively. The 112-kDa band cross-reacted with antibody 56.1 and comigrated with the band identified as immature APP<sub>751</sub> in PC-12 cells (26),

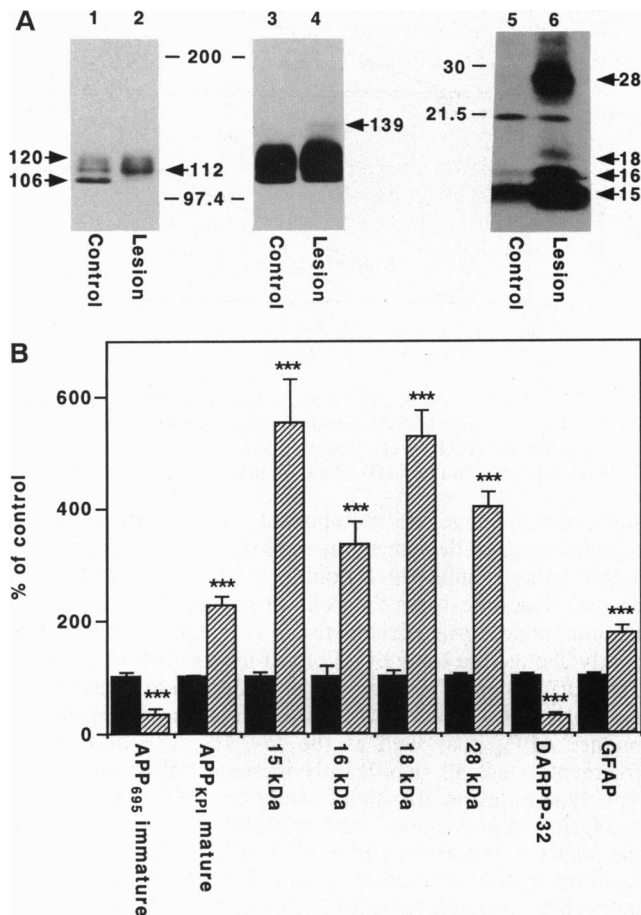


**FIG. 1.** Analysis of APP immunoreactivity in rat neostriatum after lesioning local nerve cells by quinolinic acid injection. APP bands from nonlesioned (control) and lesioned sides were analyzed 7 days after lesioning. (A) Proteins separated by NaDodSO<sub>4</sub>/PAGE in Tris/glycine (lanes 1–4) or in Tris/tricine (lanes 5 and 6) buffer. Immunoblots were exposed for 10 sec (lanes 1 and 2), 30 sec (lanes 3 and 4), or 5 min (lanes 5 and 6). The arrows at 106, 112, 120, 139, 15, 16, 18, and 28 kDa indicate putative immature APP<sub>695</sub>, immature isoform(s) of APP containing a KPI domain (APP<sub>KPI</sub>), mature APP<sub>695</sub>, mature APP<sub>KPI</sub>, and four COOH-terminal fragments of APP, respectively. The positions of molecular size markers are also indicated. (B) Tissue levels of immature APP<sub>695</sub>, mature APP<sub>KPI</sub>, APP COOH-terminal fragments (15 kDa, 16 kDa, 18 kDa, and 28 kDa), DARPP-32, and GFAP in control sides (solid bars) and lesioned sides (hatched bars). Data represent mean  $\pm$  SEM,  $n = 10$ . \*\*\*, Different from control at  $P < 0.001$  (Student's  $t$  test).

whereas the 120-kDa band did not cross-react with antibody 56.1. The 15-kDa COOH-terminal fragment most likely represents the nonamyloidogenic intra- $\beta$ /A4 cleavage product, which is the major membrane-bound APP fragment produced (28).

Additional APP species were observed in the neostriatum of rats after lesioning of local nerve cells by injection of quinolinic acid (Fig. 1A). When proteins were separated by NaDodSO<sub>4</sub>/PAGE, 15-, 16-, 18-, and 28-kDa APP immunoreactive bands were observed in Tris/glycine buffer (data not shown). These four bands migrated as 11-, 13.3-, 15.7-, and 26-kDa bands, respectively, in Tris/tricine buffer. Such aberrant migration of APP fragments has been described. APP COOH-terminal fragments from human brain, which migrate at 17 kDa in the Tris/glycine system and at 11- to 12-kDa in Tris/tricine, were shown to contain the entire  $\beta$ /A4, whereas several bands migrating at 15 kDa in Tris/glycine and at <11 kDa in Tris/tricine were nonamyloidogenic (29). In Tris/glycine buffer, the 15-kDa band from rat brain comigrated with the 15-kDa (nonamyloidogenic) band from human brain (data not shown). The COOH-terminal fragments are referred to in this report in terms of their apparent molecular mass when analyzed by NaDodSO<sub>4</sub>/PAGE with Tris/glycine buffer. When antiserum 369 was preabsorbed with synthetic APP<sub>645-694</sub> (APP<sub>695</sub> numbering), none of the bands identified as APP holofoms or APP COOH-terminal fragments was visualized. The APP COOH-terminal fragments of 15, 16, 18, and 28 kDa were also detected with an antibody raised against the COOH-terminal 15 amino acids of APP (CT15).

On the basis of earlier reports and our current results, we conclude that the 106- and 112-kDa proteins are immature (partially glycosylated) APP<sub>695</sub> and APP<sub>KPI</sub>, respectively, that the 120- and 139-kDa proteins are mature (fully glycosylated) APP<sub>695</sub> and APP<sub>KPI</sub>, respectively, that the 15-kDa band is a nonamyloidogenic COOH-terminal fragment derived from intra- $\beta$ /A4 cleavage of APP, and that the 16-, 18-, and 28-kDa bands are potentially amyloidogenic APP COOH-terminal fragments.

**Effects of Quinolinic Acid-Induced Lesions in the Striatum.** To investigate whether neuronal degeneration is associated with changes in the levels of individual APP isoforms and/or APP proteolytic fragments in the vicinity of the lesion, we examined the effects of brain lesions that destroy local (intrinsic) neurons. For this purpose, we stereotactically injected the excitotoxin quinolinic acid into the neostriatum, which results in destruction of the major population of intrinsic neurons but spares incoming nerve fibers and glial cells (30). When examined 7 days postsurgically, we found that the lesioning had no significant effect on the total level of full-length APP, as analyzed by densitometry and integration of all APP bands in the 106- to 139-kDa range (data not shown). However, analysis of individual immunoreactive bands demonstrated a considerable decrease in immature APP<sub>695</sub> [Fig. 1A (lanes 1 and 2) and B]. In contrast, increases were observed in the levels of mature APP<sub>KPI</sub> [Fig. 1A (lanes 3 and 4) and B]. Visual inspection of the autoradiograms indicated that the levels of immature APP<sub>KPI</sub> also increased. However, the changes in immature APP<sub>KPI</sub> and mature APP<sub>695</sub> could not be reliably quantitated due to difficulty in resolving them by densitometry. An increase in immature APP<sub>KPI</sub> was also observed in parallel studies using 56.1, an antibody against the KPI domain of APP (data not shown). The 15-kDa COOH-terminal fragment also increased in content, as did several potentially amyloidogenic fragments with apparent molecular masses of 16, 18, and 28 kDa [Fig. 1A (lanes 5 and 6) and B].

The quinolinic acid lesion induced a 70% decrease in DARPP-32 (Fig. 1B), a phosphoprotein enriched specifically in intrinsic neurons in the neostriatum (13, 31), indicating that

degeneration of these neurons had occurred in response to the lesion. In contrast, levels of GFAP, an astrocytic protein (32, 33), increased by 77%, indicating that gliosis had taken place (Fig. 1B).

**Correlations of the Levels of Various APP Isoforms and COOH-Terminal Fragments with the Levels of DARPP-32 and GFAP.** The levels of various APP isoforms and COOH-terminal fragments were directly compared with the level of DARPP-32. Immature APP<sub>695</sub> decreased in parallel with the loss of DARPP-32 (Fig. 2A). In contrast, the level of mature APP<sub>KPI</sub> (Fig. 2B), as well as the levels of both the 15-kDa (Fig. 2C) and 28-kDa (Fig. 2D) fragments, showed an inverse correlation with the DARPP-32 level. The levels of the various APP isoforms and COOH-terminal fragments were also compared with the GFAP level (Fig. 3). Mature APP<sub>KPI</sub> and the 15- and 28-kDa fragments increased in proportion to the increase of GFAP. In contrast, the level of immature APP<sub>695</sub> showed an inverse correlation with that of GFAP. The results shown in Figs. 2 and 3 suggest that immature APP<sub>695</sub> was derived predominantly from neurons and that mature APP<sub>KPI</sub> was derived predominantly from glial cells (cf., 9, 34–36). Moreover, we speculate that the COOH-terminal fragments resulted predominantly from increased amounts of glial APP<sub>KPI</sub> but cannot exclude the possibility that they were derived from increased processing of neuronal APP<sub>695</sub>.

**Effects in Striatum after Cortical Lesions.** To examine the question as to whether degeneration of nerve terminals is

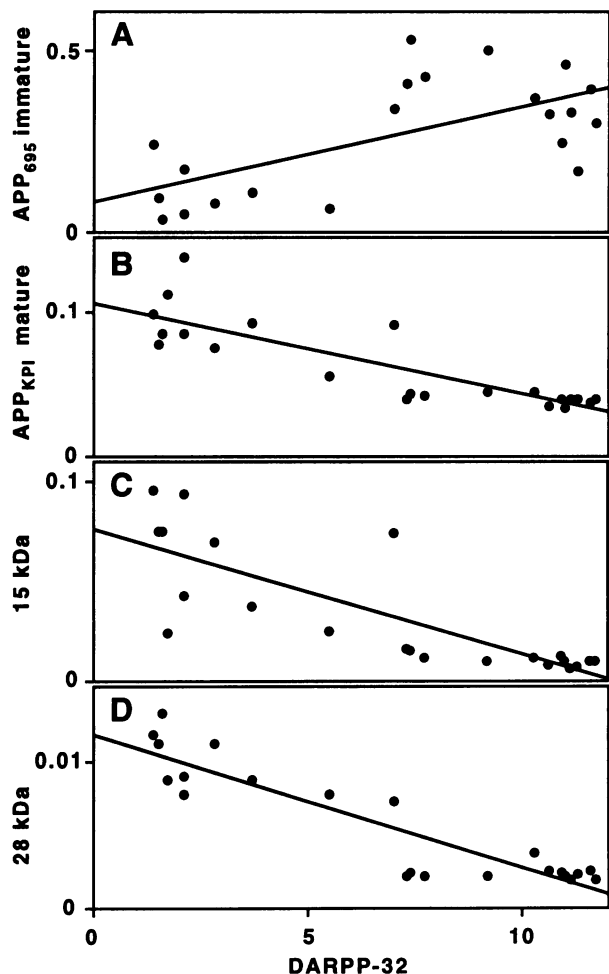


FIG. 2. Correlation of levels of immature APP<sub>695</sub> (A), mature APP<sub>KPI</sub> (B), and APP COOH-terminal fragments of 15 kDa (C) and 28 kDa (D) with levels of DARPP-32. Correlation coefficients were 0.68 (A), 0.84 (B), 0.80 (C), and 0.91 (D). Data are presented as arbitrary units.

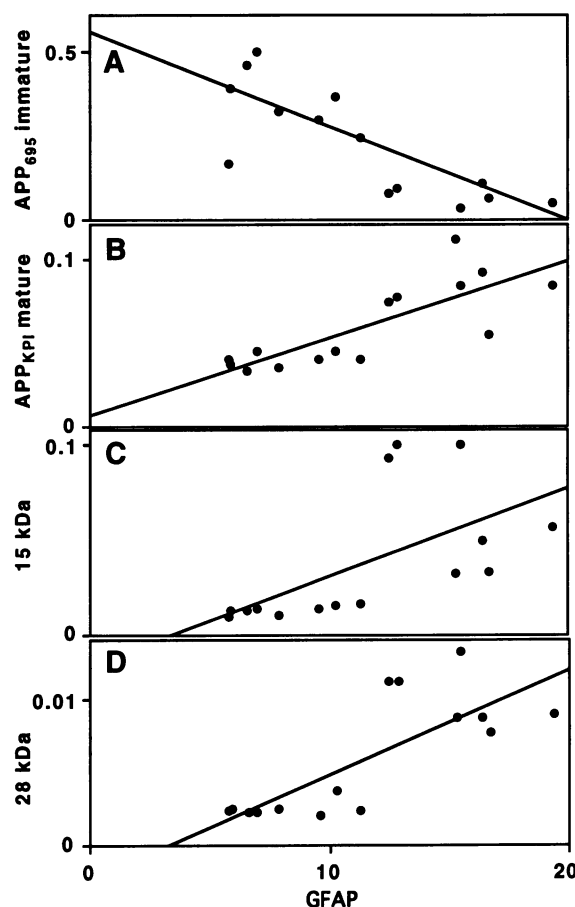


FIG. 3. Correlation of levels of immature APP<sub>695</sub> (A), mature APP<sub>KPI</sub> (B), and APP COOH-terminal fragments of 15 kDa (C) and 28 kDa (D) with GFAP levels. Correlation coefficients were 0.81 (A), 0.80 (B), 0.60 (C), and 0.78 (D). Data are presented as arbitrary units.

sufficient to change APP metabolism, we used remote lesions to induce axonal degeneration and loss of nerve terminals in target areas. Unilateral lesioning of the anterior cerebral cortex, which destroys the cells of origin of the excitatory glutamatergic corticostriatal fibers (17, 37), did not significantly change the total levels of full-length APP or of immature APP<sub>695</sub> (which presumably is present in local nerve cell bodies) in the ipsilateral neostriatum (Fig. 4). However, mature APP<sub>KPI</sub>, as well as the 15-, 16-, 18-, and 28-kDa fragments were all significantly increased after this lesion. This type of lesion also significantly decreased the levels of synapsin I, a presynaptic marker protein (38), and increased the levels of the astrocytic marker GFAP. Hence, a lesion resulting in degeneration of afferent fibers to the neostriatum induced a considerable gliosis, an increase in APP<sub>KPI</sub>, and increases in both nonamyloidogenic and putative amyloidogenic fragments in the target area.

**Effects in Substantia Nigra after Quinolinic Acid-Induced Lesions in the Striatum.** The cortical lesions destroy a predominantly excitatory neuronal pathway. We also examined the effects of degeneration of inhibitory nerve terminals. For this purpose, we used quinolinic acid lesions to destroy the predominantly  $\gamma$ -aminobutyric acid-containing striatonigral fibers (39). This lesion led to a loss of  $\approx 50\%$  of the striatonigral nerve terminals, as measured by a decrease of  $51 \pm 11\%$ ,  $P < 0.05$ , in DARPP-32 immunoreactivity in the substantia nigra and reflected in a decrease of  $41 \pm 4\%$ ,  $P < 0.001$ , in synapsin I immunoreactivity. These effects were accompanied by a decrease in mature APP<sub>695</sub>, with no apparent change in immature APP<sub>695</sub> (Fig. 5). These obser-

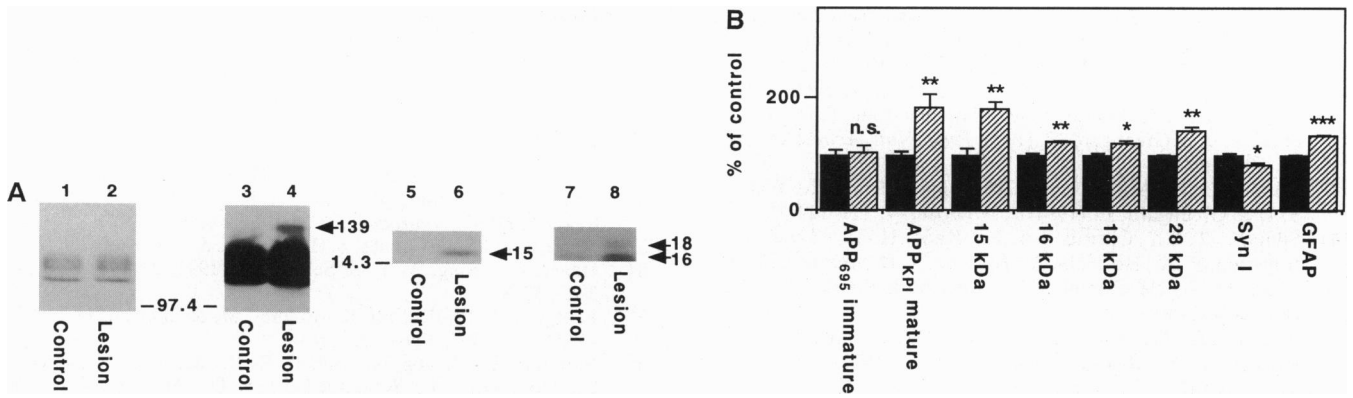


FIG. 4. Analysis of APP immunoreactivity in the neostriatum after corticostriatal nerve fiber degeneration. APP bands from nonlesioned (control) and lesioned sides were analyzed 7 days after unilateral anterior decortication. (A) Proteins were separated by NaDodSO<sub>4</sub>/PAGE in Tris/glycine (lanes 1–6) or in Tris/tricine (lanes 7 and 8) buffer. Immunoblots were exposed for 10 sec (lanes 1 and 2), 30 sec (lanes 3–6), or 10 min (lanes 7 and 8). The arrows at 139, 15, 16, and 18 kDa indicate putative mature APP<sub>KPI</sub> and three APP COOH-terminal fragments, respectively. The positions of molecular mass markers are also indicated. (B) Tissue levels of immature APP<sub>695</sub>, mature APP<sub>KPI</sub>, APP COOH-terminal fragments (15 kDa, 16 kDa, 18 kDa, and 28 kDa), synapsin I (Syn I), and GFAP in control sides (solid bars) and lesioned sides (hatched bars). Data represent mean  $\pm$  SEM,  $n = 8$ . n.s., Not significant; significantly different from control at \*,  $P < 0.05$ ; \*\*,  $P < 0.01$ ; \*\*\*,  $P < 0.001$  (Student's  $t$  test).

vations can be explained by the absence of immature APP<sub>695</sub> and the presence of mature APP<sub>695</sub> in nerve terminals (cf., 40). Lesioning of the striatonigral pathway also induced a gliosis in the substantia nigra, as measured by an increase in GFAP immunoreactivity ( $18 \pm 3\%$ ,  $P < 0.05$ ), as well as significant increases in mature APP<sub>KPI</sub> ( $33 \pm 11\%$ ,  $P < 0.05$ ) and the 16-kDa ( $31 \pm 9\%$ ,  $P < 0.05$ ) (Fig. 5) and 18-kDa ( $30 \pm 10\%$ ,  $P < 0.05$ ) (data not shown) bands.

## DISCUSSION

The present results indicate that different types of lesions in the rat brain, which induce neuronal degeneration and a concomitant gliosis, cause changes in the levels of distinct APP isoforms and proteolytic COOH-terminal fragments of APP. Destruction of neurons leads to prominent increases in APP fragments, both in the lesioned area and in those projection areas where the axons of the lesioned neurons terminate. The changes observed in the projection areas, including changes in the levels and processing of various APP isoforms, are very likely attributable to the degenerating nerve terminals. However, it is important to emphasize that neuronal degeneration is probably not sufficient to induce amyloid formation because some neurodegenerative diseases, such as Parkinson disease and Huntington disease, are

not associated with the formation of amyloid plaques in the affected areas.

It is reasonable to speculate that the changes in APP metabolism observed in the present study might be mediated through the gliotic response to neuronal degeneration. In support of this theory, microglial/macrophage invasion of the lesioned area appears to represent an early stage in lesion-induced gliosis (41). Activated microglial cells release interleukin 1 (42), which acts as a mitogen for astrocytes. Interleukin 1 has also been found to induce synthesis (43) and secretion (44) of APP. It will be important to determine, using specific antibodies against  $\beta/A4$  (cf., 45–47), whether the experimental manipulations used in the present study also stimulate the formation of amyloid. Such studies should help to determine the extent to which altered processing of APP, observed in response to nerve-terminal degeneration, reflects pathophysiological processes involved in Alzheimer disease.

We thank S. E. Gandy for valuable discussions; S. E. Gandy, J. D. Buxbaum, and G. L. Caporaso for critical reading of the manuscript; and N. C. Danbolt and L. Levy for help with the cortical lesions. This work was supported by National Institutes of Health Grants AG09464 and AG10491 (P.G.).

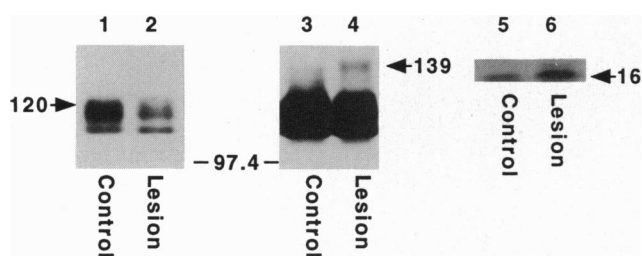


FIG. 5. Analysis of APP immunoreactivity in the substantia nigra after unilateral striatonigral nerve fiber degeneration. APP bands from nonlesioned (control) and lesioned sides were analyzed 7 days after quinolinic acid injection into the neostriatum. Proteins were separated by NaDodSO<sub>4</sub>/PAGE in Tris/glycine (lanes 1–4) or Tris/tricine (lanes 5 and 6) buffer. Tissue samples are from the same animals as those used for Fig. 1. Immunoblots were exposed for 5 sec (lanes 1 and 2), 1 min (lanes 3 and 4), or 7 min (lanes 5 and 6). The arrows at 120, 139, and 16 kDa indicate putative mature APP<sub>695</sub>, mature APP<sub>KPI</sub>, and an APP COOH-terminal fragment, respectively. The position of a 97.4-kDa molecular mass marker is also indicated.

- Kang, J., Lemaire, H. G., Unterbeck, A., Salbaum, J. M., Masters, C. L., Grzeschik, K. H., Multhaup, G., Beyreuther, K. & Müller-Hill, B. (1987) *Nature (London)* **325**, 733–736.
- Goldgaber, D., Lerman, M. I., McBride, O. W., Saffiotti, U. & Gajdusek, D. C. (1987) *Science* **235**, 877–880.
- Tanzi, R. E., Gusella, J. F., Watkins, P. C., Bruns, G. A. P., St. George-Hyslop, P., van Keuren, M. L., Patterson, D., Pagan, S., Kurnit, D. M. & Neve, R. L. (1987) *Science* **235**, 880–883.
- Robakis, N. K., Ramakrishna, N., Wolfe, G. & Wisniewski, H. M. (1987) *Proc. Natl. Acad. Sci. USA* **84**, 4190–4194.
- Ponte, P., Gonzalez-DeWhitt, P., Schilling, J., Miller, J., Hsu, D., Greenberg, B., Davis, K., Wallace, W., Lieberburg, I., Fuller, F. & Cordell, B. (1988) *Nature (London)* **331**, 525–527.
- Tanzi, R. E., McClatchey, A. I., Lamperti, E. D., Villa-Komaroff, L., Gusella, J. F. & Neve, R. L. (1988) *Nature (London)* **331**, 528–530.
- Kitaguchi, N., Takahashi, Y., Tokushima, Y., Shiojiri, S. & Ito, H. (1988) *Nature (London)* **331**, 530–532.
- Siman, R., Card, J. P., Nelson, R. B. & Davis, L. G. (1989) *Neuron* **3**, 275–285.
- Kawarabayashi, T., Shoji, M., Harigaya, Y., Yamaguchi, H. & Hirai, S. (1991) *Brain Res.* **563**, 334–338.
- Shigematsu, K., McGeer, P. L., Walker, D. G., Ishii, T. & McGeer, E. G. (1992) *J. Neurosci. Res.* **31**, 443–453.

11. Wallace, W. C., Bragin, V., Robakis, N. K., Sambamurti, K., VanderPutten, D., Merrill, C. R., Davis, K. L., Santucci, A. C. & Haroutunian, V. (1991) *Mol. Brain Res.* **10**, 173–178.
12. Buxbaum, J. D., Gandy, S. E., Cicchetti, P., Ehrlich, M. E., Czernik, A. J., Fracasso, R. P., Ramabhadran, T. V., Unterbeck, A. J. & Greengard, P. (1990) *Proc. Natl. Acad. Sci. USA* **87**, 6003–6006.
13. Ouimet, C. C., Miller, P. E., Hemmings, H. C., Jr., Walaas, S. I. & Greengard, P. (1984) *J. Neurosci.* **4**, 111–124.
14. Südhof, T. C., Czernik, A. J., Kao, H.-T., Takei, K., Johnston, P. A., Horiuchi, A., Kanazir, S. D., Wagner, M. A., Perin, M. S., De Camilli, P. & Greengard, P. (1989) *Science* **245**, 1474–1480.
15. Wunderlich, D., Lee, A., Fracasso, R. P., Mierz, D. V., Bayney, R. M. & Ramabhadran, T. V. (1992) *J. Immunol. Methods* **147**, 1–11.
16. Walaas, S. I., Girault, J.-A. & Greengard, P. (1989) *J. Mol. Neurosci.* **1**, 243–250.
17. Walaas, I. (1981) *Neuroscience* **6**, 399–405.
18. Smith, P. K., Krohn, R. I., Hermanson, G. T., Mallia, A. K., Gartner, F. H., Provenzano, M. D., Fujimoto, E. K., Goeke, N. M., Olson, B. J. & Klenk, D. C. (1985) *Anal. Biochem.* **150**, 76–85.
19. Laemmli, U. K. (1970) *Nature (London)* **227**, 680–685.
20. Schägger, H. & von Jagow, G. (1987) *Anal. Biochem.* **166**, 368–379.
21. Selkoe, D. J., Berman Podlisny, M., Joachim, C. L., Vickers, E. A., Lee, G., Fritz, L. C. & Oltersdorf, T. (1988) *Proc. Natl. Acad. Sci. USA* **85**, 7341–7343.
22. Weidemann, A., König, G., Bunke, D., Fischer, P., Salbaum, J. M., Masters, C. L. & Beyreuther, K. (1989) *Cell* **57**, 115–126.
23. Nordstedt, C., Gandy, S., Alafuzoff, I., Caporaso, G. L., Iverfeldt, K., Grebb, J. A., Winblad, B. & Greengard, P. (1991) *Proc. Natl. Acad. Sci. USA* **88**, 8910–8914.
24. Potemaska, A., Styles, J., Mehta, P., Kim, K. S. & Miller, D. L. (1991) *J. Biol. Chem.* **266**, 8464–8469.
25. Löffler, J. & Huber, G. (1992) *J. Neurochem.* **59**, 1316–1324.
26. Caporaso, G. L., Gandy, S. E., Buxbaum, J. D., Ramabhadran, T. V. & Greengard, P. (1992) *Proc. Natl. Acad. Sci. USA* **89**, 3055–3059.
27. König, G., Mönning, U., Czech, C., Prior, R., Banati, R. B., Schreiter-Gasser, U., Bauer, J., Masters, C. L. & Beyreuther, K. (1992) *J. Biol. Chem.* **267**, 10804–10809.
28. Esch, F. S., Keim, P. S., Beattie, E. C., Blacher, R. W., Culwell, A. R., Oltersdorf, T., McClure, D. & Ward, P. J. (1990) *Science* **248**, 1122–1124.
29. Estus, S., Golde, T. E., Kunishita, T., Blades, D., Lowery, D., Eisen, M., Usiak, M., Qu, X., Tabira, T., Greenberg, B. D. & Younkin, S. G. (1992) *Science* **255**, 726–728.
30. Schwarcz, R., Whetsell, W. O., Jr., & Mangano, R. M. (1983) *Science* **219**, 316–318.
31. Walaas, S. I. & Greengard, P. (1984) *J. Neurosci.* **4**, 84–98.
32. Isacson, O., Fischer, W., Victorin, K., Dawbarn, D. & Björklund, A. (1987) *Neuroscience* **20**, 1043–1056.
33. Aono, S. & Kashiwamata, S. (1990) *Med. Sci. Res.* **18**, 235–239.
34. Haass, C., Hung, A. Y. & Selkoe, D. (1991) *J. Neurosci.* **11**, 3783–3793.
35. Paul, G., Dutly, F., Frei, K., Foguet, M. & Lübbert, H. (1992) *FEBS Lett.* **307**, 329–332.
36. Mönning, U., König, G., Banati, R. B., Mechler, H., Czech, C., Gehrmann, J., Schreiter-Gasser, U., Masters, C. L. & Beyreuther, K. (1992) *J. Biol. Chem.* **267**, 23950–23956.
37. Divac, I., Fonnum, F. & Storm-Mathisen, J. (1977) *Nature (London)* **266**, 377–378.
38. De Camilli, P., Benfenati, F., Valtorta, F. & Greengard, P. (1990) *Annu. Rev. Cell Biol.* **6**, 433–460.
39. Fonnum, F. & Walaas, I. (1979) in *The Neostriatum*, eds. Divac, I. & Öberg, R. G. E. (Pergamon, New York), pp. 53–69.
40. Koo, E. H., Sisodia, S. S., Archer, D. R., Martin, L. J., Weidemann, A., Beyreuther, K., Fischer, P., Masters, C. L. & Price, D. L. (1990) *Proc. Natl. Acad. Sci. USA* **87**, 1561–1565.
41. Marty, S., Dusart, I. & Peschanski, M. (1991) *Neuroscience* **45**, 529–539.
42. Giulian, D. & Baker, T. J. (1986) *J. Neurosci.* **6**, 2163–2178.
43. Goldgaber, D., Harris, H. W., Hla, T., Maciag, T., Donnelly, R. J., Jacobsen, J. S., Vitek, M. P. & Gajdusek, D. C. (1989) *Proc. Natl. Acad. Sci. USA* **86**, 7606–7610.
44. Buxbaum, J. D., Oishi, M., Chen, H. I., Pinkas-Kramarski, R., Jaffe, E. A., Gandy, S. E. & Greengard, P. (1992) *Proc. Natl. Acad. Sci. USA* **89**, 10075–10078.
45. Haass, C., Schlossmacher, M. G., Hung, A. Y., Vigo-Pelfrey, C., Mellon, A., Ostaszewski, B. L., Lieberburg, I., Koo, E. H., Schenk, D., Teplow, D. B. & Selkoe, D. J. (1992) *Nature (London)* **359**, 322–325.
46. Seubert, P., Vigo-Pelfrey, C., Esch, F., Lee, M., Dovey, H., Davis, D., Sinha, S., Schlossmacher, M., Whaley, J., Swindlehurst, C., McGormack, R., Wolfert, R., Selkoe, D., Lieberburg, I. & Schenk, D. (1992) *Nature (London)* **359**, 325–327.
47. Shoji, M., Golde, T. E., Ghiso, J., Cheng, T. T., Estus, S., Shaffer, L. M., Cai, X.-D., McKay, D. M., Tinter, R., Frangione, B. & Younkin, S. G. (1992) *Science* **258**, 126–129.